RADIALLY VARYING MAGNETIC FIELD EFFECT ON PERISTALTIC MOTION WITH HEAT AND MASS TRANSFER OF A NON-NEWTONIAN FLUID BETWEEN TWO CO-AXIAL TUBES

by

Nabil ELDABE[a] and Mohamed ABOU-ZEID[a,b*]

[a] Department of Mathematics, Faculty of Education, Ain Shams University, Heliopolis, Cairo, Egypt

[b] Department of Mathematics, Faculty of Science, University of Tabuk, Tabuk, Saudi Arabia

Original scientific paper
https://doi.org/10.2298/TSCI160409292E

The present analysis discusses the effects of thermal-diffusion with thermal radiation, Joule heating and internal heat generation on peristaltic flow of a non-Newtonian fluid obeying Jeffery model. Heat and mass transfer are also taken into consideration, the flow is between two co-axial tubes under the effect of radially varying magnetic field. The inner tube is uniform and at rest, while the outer tube is flexible with sinusoidal wave traveling. The problem is modulated mathematically by a system of partial differential equations which describes the equations of momentum, heat, and mass transfer. These equations are solved analytically under the assumptions of long wave length and low-Reynolds number in non-dimensional form. The solutions are obtained as a functions of physical parameters of the problem. The radially varying magnetic field effect on the temperature and concentration distributions is analyzed and it is shown that the increase of Hartman number tends to reduce the temperature, while it increases the concentration.

Key words: *non-Newtonian fluid, peristaltic flow, magnetohydrodynamic, heat and mass transfer*

Introduction

An important mechanism for mixing and transporting fluids is peristalsis which is generated by a progressive wave of contraction or expansion moving on the wall of the tube. The continuous periodic muscular oscillations of the ducts pumped the physiological fluids in animal and human bodies. The progressive transverse contraction waves that propagate along the walls of the ducts causes these oscillations. Peristaltic flow occurs widely in the functioning of the ureter, food mixing and chime movement in the intestine, movement of eggs in the fallopian tube, the transport of the spermatozoa in cervical canal, transport of bile in the bile duct, transport of cilia, and circulation of blood in small blood vessels [1]. Peristaltic flows have been the subject of many researchers because of its applications in physiology and industry. Akram *et al.* [2] have obtained numerical and analytical solutions of the peristaltic flow of Williamson fluid in the occurrence of induced magnetic field. The effects of entropy and induced magnetic field for the peristaltic flow of copper water fluid in the asymmetric horizontal channel have been investigated by Akbar *et al.* [3]. Nadeem and Akbar [4] discussed the peristaltic flow of Walter's B fluid in a uniform inclined tube. The effects of magnetic field and heat transfer on the

* Corresponding author, e-mail: master_math2003@yahoo.com

peristaltic flow of an incompressible couple stress fluid through porous medium in an inclined asymmetric channel have been studied by Ramesh and Devakar [5]. Eldabe and Abou-zeid [6] discussed the peristaltic transport of a micropolar non-Newtonian fluid through a porous media between two co-axial tubes with heat and mass transfer under long-wavelength assumption. Hayat *et al.* [7] analyzed the problem of MHD peristaltic transport of nanofluid in a channel with wall properties in the presence of viscous dissipation, partial slip, and Joule heating effects. Recently, many authors reported analytical and numerical studies of peristaltic flow of Newtonian and non-Newtonian fluids [8-12].

The problems heat with mass transfer have achieved great importance in many processes and have, therefore, received a considerable amount of attention in recent years. In processes such as drying, evaporation at the surface of a water body, energy transfer in a wet cooling tower and the flow in a desert cooler, heat and mass transfer occurs simultaneously. Possible applications of this type of flow can be found in many industries. Many practical diffusive operations which involve the molecular diffusion of a species are discussed in [13]. Akbar *et al.* [14] obtained exact solutions of the problem of heat generation effects on MHD peristaltic motion in permeable tube under the assumption of long-wavelength and low-Reynolds number. Because of the importance of applications of peristaltic flow with heat and mass transfer, many investigators have studied such flows [4, 15-19].

Effects of a variable magnetic field on the peristaltic flow of a Jeffrey fluid in a tube are studied by Abd-Alla *et al.* [20]. They obtained exact analytical solutions of the governing equations which were simplified under the consideration of long wavelength and low Reynolds number approximation. The main aim of this study is to extend the work of Abd-Alla *et al.* [20] to include the heat and mass transfer equations with the effects of Joule heating, thermal radiation, and internal heat generation. The analytical solutions of these equations are obtained under the assumptions of long wavelength and low-Reynolds number. These solutions are expressed in terms of special functions which involve the physical parameters of the problem. Effects of these parameters on solutions are discussed numerically and graphically to show the relations between parameters and solutions and to show how we can control solutions by changing parameters. We think that this study has a wide range of practical importance in many scientific fields such as biological, chemical, medical, and industrial fields.

Mathematical model

Consider a non-Newtonian fluid saturated between two co-axial annuli with internal radius r_1 and external radius r_2. The inner tube is uniform and at rest, while the outer tube has a sinusoidal wave traveling. The system is stressed by a varying magnetic field $\underline{B}(r)$ which acts on the azimuthal direction. A cylindrical co-ordinates system (r,θ,z) is considered; the geometry of the wall surfaces is described in fig. 1 and the equations for the radii are:

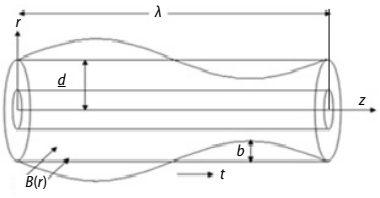

Figure 1. Schematic of the problem

$$r_1 = a_1 \tag{1}$$

$$r_2 = H = d + \bar{b}\sin\frac{2\pi}{\lambda}(z - ct) \tag{2}$$

The constitutive equations for an incompressible Jeffry fluid are given:

$$\underline{\boldsymbol{\tau}} = -P\mathbf{I} + \underline{\mathbf{S}} \tag{3}$$

$$\underline{S} = \frac{\mu}{1+\lambda_1}(\dot{\gamma} + \lambda_2 \ddot{\gamma}) \tag{4}$$

The parameters of flow are independent of the azimuthal co-ordinate θ, so, the velocity is given by $\underline{V} = (u, 0, w)$. The magnetic field $\underline{B}$ generated by the electric current J is given by Biot-Savart law:

$$B = B_0 \frac{r_1}{r}, \quad B_0 = \frac{\mu_0 J}{2\pi r_1} \tag{5}$$

The governing equations for an incompressible flow in the fixed frame are given [6]:

$$\frac{\partial u}{\partial r} + \frac{u}{r} + \frac{\partial w}{\partial z} = 0 \tag{6}$$

$$\rho\left(u\frac{\partial u}{\partial r} + w\frac{\partial u}{\partial z}\right) = -\frac{\partial P}{\partial r} + \frac{1}{1+\lambda_1}\left(\frac{\partial^2 u}{\partial r^2} + \frac{1}{r}\frac{\partial u}{\partial r} - \frac{u}{r^2} + \frac{\partial^2 u}{\partial z^2}\right) - \frac{\sigma B_0^2}{r^2}u \tag{7}$$

$$\rho\left(u\frac{\partial w}{\partial r} + w\frac{\partial w}{\partial z}\right) = -\frac{\partial P}{\partial z} + \frac{1}{1+\lambda_1}\left(\frac{\partial^2 w}{\partial r^2} + \frac{1}{r}\frac{\partial w}{\partial r} - \frac{\partial^2 w}{\partial z^2}\right) - \frac{\sigma B_0^2}{r^2}w \tag{8}$$

$$\rho c_p\left(u\frac{\partial T}{\partial r} + w\frac{\partial T}{\partial z}\right) = k\left(\frac{\partial^2 T}{\partial r^2} + \frac{1}{r}\frac{\partial T}{\partial r} + \frac{\partial^2 T}{\partial z^2}\right) - \frac{1}{r}\frac{\partial (rq_r)}{\partial r} + \frac{\sigma B_0^2}{r^2}\left(u^2 + w^2\right) + Q_0\left(T - T_2\right) \tag{9}$$

$$u\frac{\partial C}{\partial r} + w\frac{\partial C}{\partial z} = D\left(\frac{\partial^2 C}{\partial r^2} + \frac{1}{r}\frac{\partial C}{\partial r} + \frac{\partial^2 C}{\partial z^2}\right) + \frac{Dk_T}{T_2}\left(\frac{\partial^2 T}{\partial r^2} + \frac{1}{r}\frac{\partial T}{\partial r} + \frac{\partial^2 T}{\partial z^2}\right) \tag{10}$$

The boundary conditions are given:

$$u = 0, \quad w = 0, \quad T = T_1, \quad C = C_1 \quad \text{at} \quad r = r_1 \tag{11}$$

$$u = -c\frac{\partial H}{\partial z}, \quad w = -c, \quad T = T_2, \quad C = C_2 \quad \text{at} \quad r = r_2 \tag{12}$$

By using Rosseland approximation [21], the radiative heat flux is given:

$$q_r = \frac{-4\sigma^*}{3k_R}\frac{\partial T^4}{\partial r} \tag{13}$$

it is assumed that the temperature differences within the flow are sufficiently small such that T^4 may be expressed as a linear function of temperature. This is accomplished by expanding T^4 in a Taylor series about T_2 and neglecting higher-order terms, one gets:

$$T^4 \approx 4T_2^3 T - 3T_2^4 \tag{14}$$

The appropriate non-dimensional variables for the flow are defined:

$$\begin{gathered} r^* = \frac{r}{d}, \quad z^* = \frac{z}{\lambda}, \quad u^* = \frac{\lambda}{cd}u, \quad w^* = \frac{w}{c}, \quad P^* = \frac{d^2}{\lambda c\mu}P, \quad T^* = \frac{T - T_2}{T_1 - T_2} \\ \delta = \frac{d}{\lambda}, \quad Q_0{}^* = \frac{Q_0 d}{\rho c_p c}, \quad C^* = \frac{C - C_2}{C_1 - C_2}, \quad t^* = \frac{c}{\lambda}t, \quad h = \frac{H}{d}, \quad \varepsilon = \frac{a_1}{d}, \quad \varphi = \frac{b}{d} \end{gathered} \tag{15}$$

In terms of these variables, dropping the star mark for simplicity and taking into account long wavelength and low-Reynolds number approximation, eqs. (6)-(10) become:

$$\frac{\partial u}{\partial r}+\frac{u}{r}+\frac{\partial w}{\partial z}=0 \tag{16}$$

$$\frac{\partial P}{\partial r}=0 \tag{17}$$

$$\frac{\partial P}{\partial z}=\frac{1}{1+\lambda_1}\left(\frac{\partial^2 w}{\partial r^2}+\frac{1}{r}\frac{\partial w}{\partial r}-\frac{\partial^2 w}{\partial z^2}\right)-\frac{\mathrm{M}^2}{r^2}w \tag{18}$$

$$\left(\frac{3+4R}{3\,\mathrm{Pr}}\right)\left(\frac{\partial^2 T}{\partial r^2}+\frac{1}{r}\frac{\partial T}{\partial r}\right)+\frac{\mathrm{Ec}\,\mathrm{M}^2}{r^2}w^2+Q_0 T=0 \tag{19}$$

$$\frac{\partial^2 C}{\partial r^2}+\frac{1}{r}\frac{\partial C}{\partial r}+\mathrm{Sc}\,\mathrm{Sr}\left(\frac{\partial^2 T}{\partial r^2}+\frac{1}{r}\frac{\partial T}{\partial r}\right)=0 \tag{20}$$

Thus, the boundary conditions, eqs. (11) and (12), in their dimensionless form read:

$$u=0,\quad w=0,\quad T=C=0\quad \text{at}\quad r=\varepsilon \tag{21}$$

$$u=-\frac{\partial h}{\partial z},\quad w=-1,\quad T=C=1\quad \text{at}\quad r=h=1+\varphi \tag{22}$$

Exact solution

This section presents the exact solutions of the system of eqs. (18)-(20) with boundary conditions, eqs. (21) and (22), the axial velocity, temperature and concentration can be written:

$$w(r,z)=\alpha_1 r^a+\alpha_2 r^{-a}+\alpha_3 r^{2+2a}+\alpha_4 r^{2-2a}+\alpha_5 r^2 \tag{23}$$

$$\begin{aligned}T(r,z)=&\alpha_6 J_0(br)+\alpha_7 Y_0(br)+\\&+Y_0(br)\left[\alpha_8 r^2 J_0(br)+\alpha_9 r J_0(br)J_1(br)+\alpha_{10} r^2 J_2(br)+\alpha_{11} r^3 J_3(br)\right]+\\&+rJ_0(br)Y_1(br)\left[\alpha_{12}+\alpha_{13} r^2+\alpha_{14} J_0(br)\right]+\\&+\alpha_{15} r^{1-2a} J_0(br)Y_1(br)\,{}_1F_2\left(1;\,1-a,\,1-a;\,-\frac{1}{4}b^2r^2\right)+\\&+\alpha_{16} r^{-2a} J_0(br)Y_0(br)\,{}_1F_2\left(1;\,1-a,\,-a;\,-\frac{1}{4}b^2r^2\right)+\\&+\alpha_{17} r^{2-a} J_0(br)Y_0(br)\,{}_1F_2\left(1;\,1-\frac{a}{2},\,2-\frac{a}{2};\,-\frac{1}{4}b^2r^2\right)+\\&+\alpha_{18} r^{3-a} J_0(br)Y_1(br)\,{}_1F_2\left(1;\,2-\frac{a}{2},\,2-\frac{a}{2};\,-\frac{1}{4}b^2r^2\right)+\\&+\alpha_{19} r^{2+a} J_0(br)Y_0(br)\,{}_1F_2\left(1;\,1+\frac{a}{2},\,2+\frac{a}{2};\,-\frac{1}{4}b^2r^2\right)+\\&+\alpha_{20} r^{3+a} J_0(br)Y_1(br)\,{}_1F_2\left(1;\,2+\frac{a}{2},\,2+\frac{a}{2};\,-\frac{1}{4}b^2r^2\right)+\end{aligned}$$

$$+\alpha_{21}r^{2a}J_0(br)Y_0(br)_1F_2(1;\ a,\ 1+a;\ -\frac{1}{4}b^2r^2)+$$

$$+\alpha_{22}r^{1+2a}J_0(br)Y_1(br)_1F_2(1;\ 1+a,\ 1+a;\ -\frac{1}{4}b^2r^2)+$$

$$+\alpha_{23}r^{2-a}Y_0(br)_1F_2(1-\frac{a}{2};\ 1,\ 2-\frac{a}{2};\ -\frac{1}{4}b^2r^2)+$$

$$+\alpha_{24}r^{2+a}Y_0(br)_1F_2(1+\frac{a}{2};\ 1,\ 2+\frac{a}{2};\ -\frac{1}{4}b^2r^2)+$$

$$+\alpha_{25}r^{-2a}Y_0(br)_1F_2(-a;\ 1,\ 1-a;\ -\frac{1}{4}b^2r^2)+$$

$$+\alpha_{26}r^{2a}Y_1(br)_1F_2(a;\ 1,\ 1+a;\ -\frac{1}{4}b^2r^2)$$

$$\alpha_{27}Y_0(br)G_{13}^2\left(\frac{1}{4}b^2r^2,\frac{1}{2}\Big|_{0,0,0}^{1}\right)+\alpha_{28}J_0(br)G_{24}^3\left(\frac{1}{4}b^2r^2,\frac{1}{2}\Big|_{0,0,0,\frac{-1}{2}}^{\frac{-1}{2},1}\right) \tag{24}$$

$$C(r,z)=\frac{1+\mathrm{Sc}\,\mathrm{Sr}}{\ln(2h)}\ln(2r)-\mathrm{Sc}\,\mathrm{Sr}T(r,z) \tag{25}$$

where

$$a^2=\mathrm{M}^2\left(1+\lambda_1\right)\quad\text{and}\quad b^2=\frac{3\,\mathrm{Pr}\,Q_0}{3+4R}$$

Here J_0, J_1, and J_2, are Bessel functions of the first kind of order 0, 1 and 2, respectively, and Y_0 and Y_1 are Bessel functions of the second kind of order 0 and 1, respectively. In eq. (24), G_{13}^2 and G_{24}^3 are Meijer functions. The mathematical formulas of the constants α_1-α_{28} are not included here. However, they are available upon request from the author.

The instantaneous volume flow rate, in the fixed frame, is given:

$$Q^*(z,t)=2\pi\int_0^h rw\,\mathrm{d}r \tag{26}$$

where the dimensionless flux, $Q=Q^*/(\pi d^2c)$, is given:

$$Q(z,t)=2\int_0^h rw\,\mathrm{d}r \tag{27}$$

Now, Nusselt number and Sherwood number at the outer annulus are defined, respectively:

$$\mathrm{Nu}=\left.\frac{\partial\theta}{\partial r}\right|_{r=h},\ \mathrm{Sh}=\left.\frac{\partial C}{\partial r}\right|_{r=h} \tag{28}$$

Numerical results and discussion

The closed solutions of this problem have been obtained analytically through the function DSolve and Solve of Mathematica package, and the results are discussed in this section. The following values of human small intestine parameters are used [6]:

$$d = 1.2 \text{ cm}, \quad c = 2 \text{ cm/min}, \quad \lambda = 8.1 \text{ cm}.$$

Since Abd-Alla *et al.* [20] have studied in details the effects of flow parameters on the velocity, our interest in this work is to study the influences of various parameters such as Hartman number, the ratio of relaxation to retardation times λ_1, the radiation parameter R, Eckert number Ec, Prandtl number Pr, Schmidt number Sc and the volumetric rate of heat generation Q_0 only on the temperature T, concentration C, Nusselt number Nu and Sherwood number Sh.

In fig. 2, a 3-D diagram is drawn to illustrate the effects of radial co-ordinate r and axial co-ordinate z on the temperature T. It is clear from this figure that the temperature decreases with increasing z, while it increases as r increases till a maximum value, and then it decreases till minimum value. The effects of Eckert number and Hartman number on the temperature T which is a function of the radial co-ordinate r are illustrated in figs. 3 and 4, respectively. The graphical results of figs. 3 and 4 indicate that the temperature increases with increasing in the parameter Ec, while it decreases by increasing the parameter M, but near boundary of outer tube, the temperature quietly increases as parameter M increases, namely in a small region $1.1 \leq r \leq \leq 1.2$.. This occurs due to opposing nature of applied magnetic field with respect to the flow. The following interprets the variation of heat transfer with the magnetic field. It is well-known that magnetism is created by the

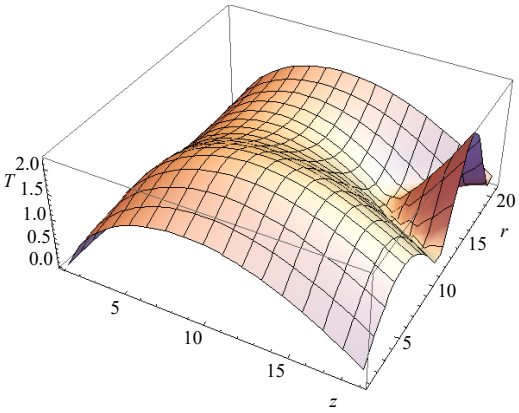

Figure 2. Three-dimensional axial velocity is plotted *vs.* r and z for a system have the particulars, M = 2, $\lambda_1 = 1.5$, dP/d$z = 5$, $z = 0.3$, Pr = 1.5, Ec = 5.5, $Q_0 = 1$, and $\varepsilon = 0.25$; the figure indicates the relation (24) (*for color image see journal web site*)

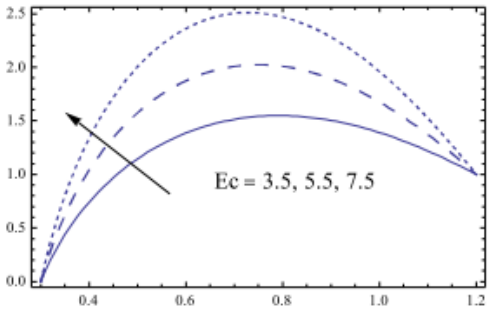

Figure 3. The temperature is plotted *vs.* r for different values of and for a system have the particulars M = 2, $\lambda_1 = 1.5$, dP/d$z = 5$, $z = 0.3$, Pr = 1.5, $Q_0 = 1$, and $\varepsilon = 0.25$; the figure indicates the relation (24)

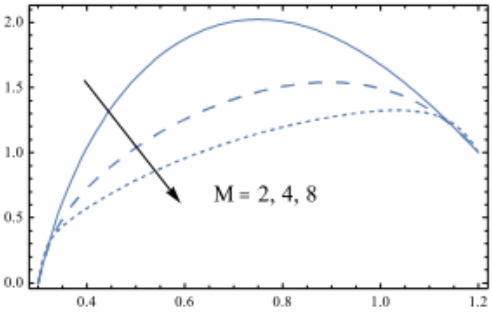

Figure 4. The temperature is plotted *vs.* r for different values of M and for a system have the particulars $\lambda_1 = 1.5$, dP/d$z = 5$, $z = 0.3$, Pr = 1.5, Ec = 5.5, $Q_0 = 1$, and $\varepsilon = 0.25$; the figure indicates the relation (24)

alignment of small domains within a specific set of metal. These domains function as all atoms do, thus the temperature affects the movement, weak magnetic field leads to high temperature. In contrast, cold temperature slows the movement (magnetic field strength and low temperatures). Slower movement leads to more fixed directions in terms of the domains. Also, the effect of viscous dissipation manufactures heat due to friction among the fluid particles, this additional force causes an increament of the initial fluid temperature, and then, the buoyant force.

It is also noted that the temperature T increases with r till a definite value $r = r_0$ (represents the maximum T) and it decreases afterwards. This maximum value of T increases by decreasing M, increasing Ec, and it occurs at another value $r > r_0$. It is also observed from fig. 3, that there is a rise in the temperature due to the heat created by the source. It agrees qualitatively with expectations; since the effect of source and dissipation temperature increases the rate of energy transport to the fluid and accordingly increases the fluid temperature. The results in fig. 3 are consistent with those obtained by Abou-Zeid [8], Eldabe and Abou-Zeid [6], and Hayat *et al.* [7]. The behavior of T with Q_0 is found to be exactly similar to the curves in fig. 4. The effects of other parameters on the temperature are found to be similar to them, but figures are excluded to avoid any kind of repetition.

The distributions of concentration C within the radial co-ordinate r for various values of Hartman number and the volumetric rate of heat generation Q_0 are exhibited in figs. (5) and (6), respectively. It is seen from figs. 5 and 6, that the concentration increases as M increases, while it decreases as Q_0 increases, but the concentration decreases with the increase of M in a small regions near the boundary of the inner and outer tubes, namely $0.3 \leq r \leq 0.35$, and $1.1 \leq r \leq 1.2$. It is also observed that the concentration for different values of M and Q_0 decreases by increasing r till a minimum value (at a finite value of $r : r = r_0$) after which it increases. The effects of Sc, Ec, and Pr on C are found to be similar to the effects of Q_0 in fig. 6. Also, the effect of λ_1 on C is found to be similar to the effect of M on C which is illustrated in fig. 5, with the only difference that the obtained curves are very close to those obtained in fig. 5, but the figure will not be given there to save space.

Tables 1 and 2, present numerical results for the quantities of Nusselt number and Sherwood number for various values of all parameters when ε is less than 1. It is clear from tab. 1 that an increase in Hartman number and Eckert number gives an increase in the values of quantity Sh but decreases the dimensionless quantity Nu. Also, an increase in the ratio of relax-

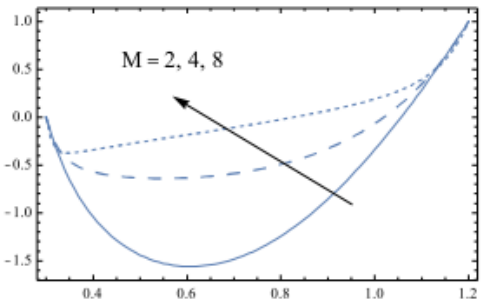

Figure 5. The concentration is plotted *vs. r* for different values of M and for a system have the particulars $\lambda_1 = 1.5$, dP/d$z = 5$, $z = 0.3$, Pr = 1.5, Ec = 5.5, $Q_0 = 1$, and $\varepsilon = 0.25$; the figure indicates the relation (24)

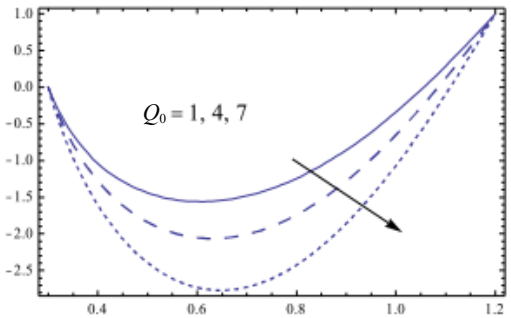

Figure 6. The concentration is plotted *vs. r* for different values of Q_0 and for a system have the particulars M = 2, $\lambda_1 = 1.5$, dP/d$z = 5$, $z = 0.3$, Pr = 1.5, Ec = 5.5, and $\varepsilon = 0.25$; the figure indicates the relation (24)

Table 1. Values of Nu and Sh for various values of M, and Ec

M	λ_1	Ec	Nu	Sh
2	1.5	5.5	–3.2303	6.92191
3	1.5	5.5	–3.74422	7.6928
4	1.5	5.5	–4.29244	8.51512
4	0.5	5.5	–5.50803	10.3385
4	2	5.5	–3.94249	7.99019
4	2.5	5.5	–3.67314	7.58617
2	2.5	4.5	–2.30667	5.53646
2	2.5	3.5	–1.63682	4.53169
2	2.5	2.5	–0.966977	3.52692

Table 2. Values of Nu and Sh for various values of Pr, R, Q_0, and Sc

Pr	R	Q_0	Sc	Nu	Sh
1.5	1.5	1	1.5	–0.966977	3.52692
2.5	1.5	1	1.5	–2.20783	5.3882
2.5	1.5	2	1.5	–2.53475	5.87858
3.5	1.5	2	1.5	–4.0263	8.11591
3.5	1.5	3	1.5	–4.6322	9.02476
3.5	1.5	2.5	1.5	–4.32037	8.55702
1.5	2.5	2.5	2.5	–0.562607	4.31356
1.5	3.5	2.5	3.5	–0.225751	4.52775
1.5	3.5	2.5	4.5	–0.225751	5.58409

ation to retardation times λ_1 gives an opposite behavior to both M and Ec. The values of both Nu and Sh for various values of Prandtl number Pr, the radiation parameter R, Schmidt number Sc and the volumetric rate of heat generation Q_0 are presented in tab. 2. It is noted that an increase in both Pr and Q_0 decreases the values of dimensionless quantity Nu, but gives an increase in the values of Sh. Also, an increase in R increases the values of dimensionless quantities Nu and Sh. But an increase in Sc gives an increase in the values of dimensionless quantity Sh but has no effect on Nu.

Conclusions

In this paper, analytical solutions of the peristaltic flow with heat and mass transfer of a Jeffery fluid between two coaxial annuli are obtained under the considerations of long wavelength and low-Reynolds number. The effects of radially varying magnetic field, radiation, Joule heating and internal heat generation are taken into account. This study is an extension of the work of Abd-Alla *et al.* [20]. The analytical expressions are constructed for the axial velocity, temperature and concentration distributions in case of constant pressure gradient. The mechanics of many physiological flows can be interpreted by the model of present analysis. Numerical calculations are presented for physical quantities of interest and their dependence on the active parameters of the fluid. The effects of these parameters are tabulated and discussed by a set of graphs. key points are summarized.

- The temperature increases with the increase each of Ec, Pr and Q_0, but it decreases as M, λ_1 and R increase.
- The temperature for different values of Ec, Pr, Q_0, M, λ_1 and R becomes greater with increasing the radial co-ordinate r and reaches maximum at $r = 0.7$.
- The concentration behavior is contrary with respect to the temperature behavior except that it decreases as Sc increases.
- Nusselt number increases, by increasing each of λ_1, R, Nb and Nt whilst it decreases as Ec, Pr, Q_0 and M increases.
- Sherwood number has an opposite behavior compared to Nusselt number.

Nomenclature

a_1 – radius of the inner tube, [m]
b – wave amplitude, [scalar]
C – fluid concentration, [kgm^{-3}]
C_1 – concentration at $r = r_1$, [kgm^{-3}]
C_2 – concentration at $r = r_2$, [kgm^{-3}]
c – propagation velocity along z-direction
c_p – specific heat at constant pressure
D – coefficient of mass diffusivity
d – radius of the outer tube, [m]
Ec – Eckert number, [$= c^2/c_P(T_1 - T_2)$], [–]

$\boldsymbol{I}$ – identity tensor
J – electric current
k – thermal conductivity
k_R – mean absorption coefficient
k_T – thermal diffusion ratio
M – Hartman number, $(= B_0 d\sqrt{\sigma/\mu_0})$, [–]
P – fluid pressure, [kgm^{-1}s^{-2}]
Pr – Prandtl number, $(= \mu c_P/k)$, [–]
Q_0 – volumetric rate of heat generation
q_r – radiative heat flux
R – radiation parameter, $(= 4\sigma^* T_2^3/kk_R)$
Re – Reynolds number
r – radial co-ordinate, [m]
$\underline{\boldsymbol{S}}$ – extra stress tensor, [tensor]
Sc – Schmidt number, $(= \mu/\rho D)$, [–]
Sr – Soret number, $\{= [Dk_T\rho(T_1 - T_2)]/[\mu_B T_2(C_1 - C_2)]\}$, [–]
T – fluid temperature
T_1 – temperature at $r = r_1$
T_2 – temperature at $r = r_2$
t – time, [s]
u – radial velocity, [ms^{-1}]
w – axial velocity, [ms^{-1}]
z – axial co-ordinate, [m]

Greek symbols

$\dot{\gamma}$ – shear rate
θ – azimuthal co-ordinate
λ – wavelength
λ_1 – ratio of relaxation to retardation times
λ_2 – retardation time
μ – viscosity of the fluid
μ_0 – magnetic permeability
ρ – fluid density
$(\rho c)_p$ – effective heat capacity of the nanoparticle material
σ – electrical conductivity
σ^* – Stefan-Boltzmann constant
$\underline{\boldsymbol{\tau}}$ – stress vector, [vector]
φ – amplitude ratio

Superscripts and subscripts

$\cdot$ – first derivative (with respect to time)
$\cdot\cdot$ – second derivative (with respect to time)

References

[1] Eldabe, N. T., *et al*., Wall Properties Effect on the Peristaltic Motion of a Coupled Stress Fluid with Heat and Mass Transfer through a Porous Medium, *J. Eng. Mech., 142* (2015), 3, 04015102
[2] Akram, S., *et al*., Numerical and Analytical Treatment on Peristaltic Flow of Williamson Fuid in the Occurrence of Induced Magnetic Feld, *J. Magn. Magn. Mater., 346* (2013), Nov., pp. 142-151
[3] Akbar, N. S., *et al*., Peristaltic Flow with Thermal Conductivity of H_2O + Cu Nanofluid and Entropy Generation, *Results Phys., 5* (2015), pp. 115-124
[4] Nadeem, S. Akbar, N. S., Peristaltic Flow of Walter's B Fuid in a Uniform Inclined Tube, *J. Biorheology, 24* (2010), 1, pp. 22-28
[5] Ramesh, K., Devakar, M., Magnetohydrodynamic Peristaltic Transport of Couple Stress Fluid through Porous Medium in an Inclined Asymmetric Channel with Heat Transfer, *J. Magn. Magn. Mater., 394* (2015), Nov., pp. 335-348
[6] Eldabe, N. T., Abou-Zeid, M. Y., Magnetohydrodynamic Peristaltic Flow with Heat and Mass Transfer of Micropolar Biviscosity Fluid through a Porous Medium between Two Co-Axial Tubes, *Arab. J. Sci. Eng., 39* (2014), 6, pp. 5045-5062
[7] Hayat, T., *et al.*, Simultaneous Effects of Slip and Wall Properties on MHD Peristaltic Motion of Nanofluid with Joule Heating, *J. Magn. Magn. Mater., 395* (2015), Dec., pp. 48-58
[8] Abou-Zeid, M. Y., Homotopy Perturbation Method to MHD Non-Newtonian Nanofluid Flow through a Porous Medium in Eccentric Annuli with Peristalsis, *Thermal Science, 21* (2017), 5, pp. 2069-2080
[9] Ellahi, R., Hussain, F., Simultaneous Effects of MHD and Partial Slip on Peristaltic Flow of Jeffery Fluid in a Rectangular Duct, *J. Magn. Magn. Mater., 393* (2015), Nov., pp. 284-292
[10] Ellahi, R., *et al*., Effects of Hall and Ion Slip on MHD Peristaltic Flow of Jeffrey Fluid in a Non-Uniform Rectangular Duct, Int. *J. Numer. Methods Heat Fluid Flow, 26* (2016), 6, pp. 1802-1820
[11] Ellahi, R., *et al*., Peristaltic Flow of Couple Stress Fluid in a Non-Uniform Rectangular Duct Having Compliant Walls, *Commun. Theor. Phys., 65* (2016), 1, pp. 66-72
[12] Khan A. A., *et al*., Bionic Study of Variable Viscosity on MHD Peristaltic Flow of Pseudoplastic Fluid in an Asymmetric Channel, *J. Magn., 21* (2016), 2, pp. 273-280
[13] Hines, A. L., Maddox, R. N., *Mass Transfer Fundamentals and Application*, Prentice Hall, N. J., USA, 1985
[14] Akbar, N. S., *et al*., Copper Oxide Nanoparticles Analysis with Water as Base Fluid for Peristaltic Flow in Permeable Tube with Heat Transfer, *Comput. Methods Programs Biomed., 130* (2016), July, pp. 22-30
[15] Vafai, K., *et al.*, The Study of Hall Current on Peristaltic Motion of a Non-Newtonian Fluid with Heat Transfer and Wall Properties, *Z. Naturforsch A., 70* (2015), pp. 281-293

[16] Akbar, N. S., *et al*., Influence of Induced Magnetic Field and Heat Flux with the Suspension of Carbon Nanotubes for the Peristaltic Flow in a Permeable Channel, *J. Magn. Magn. Mater., 381* (2015), May, pp. 405-415
[17] Akbar, N. S., Nadeem, S., Characteristics of Heating Scheme and Mass Transfer on the Peristaltic Flow for an Eyring-Powell Fluid in an Endoscope, *Int. J. Heat Mass Transfer, 55* (2012), 1-3, pp. 375-383
[18] Abd-Alla, A. M., *et al*., Influence of Heat and Mass Transfer, Initial Stress and Radially Varying Magnetic Field on the Peristaltic Flow in an Annulus with Gravity Field, *J. Magn. Magn. Mater., 363* (2015), Aug., pp. 166-178
[19] Ellahi, R., *et al*., Effects of Heat and Mass Transfer on Peristaltic Flow in a Non-Uniform Rectangular Duct, *Int. J. Heat Mass Transfer, 71* (2014), Apr., pp. 706-719
[20] Abd-Alla, A. M., *et al*., Peristaltic Flow of a Jeffrey Fluid under the Effect of Radially Varying Magnetic Field in a Tube with an Endoscope, *J. Magn. Magn. Mater., 384* (2015), June, pp. 79-86
[21] Rohsenow, W. M., *et al*., *Handbook of Heat Transfer*, McGraw-Hill Companies, New York, USA, 1998

Paper submitted: April 9, 2016
Paper revised: November 18, 2016
Paper accepted: November 26, 2016